European Journal of Chemistry

View Journal Online
View Article Online

A square planar copper(II) complex noncovalently conjugated with a *p*-cresol for bioinspired catecholase activity

Subham Mukherjee [1,2], Gayetri Sarkar [1], Abhranil De [3] and Bhaskar Biswas [1,*]

[1] *Department of Chemistry, University of North Bengal, Darjeeling, 734013, India*
[2] *Department of Chemistry, Surya Sen Mahavidyalaya, Jalpaiguri, 734004, India*
[3] *Department of Basic Science and Humanities, Hooghly Engineering and Technology College, Hooghly, 712103, India*

* *Corresponding author at: Department of Chemistry, University of North Bengal, Darjeeling, 734013, India.*
e-mail: bhaskarbiswas@nbu.ac.in (B. Biswas).

RESEARCH ARTICLE

10.5155/eurjchem.14.4.499-506.2489

Received: 28 October 2023
Received in revised form: 04 December 2023
Accepted: 10 December 2023
Published online: 31 December 2023
Printed: 31 December 2023

KEYWORDS

Single crystal
X-ray structure
Characterization
Copper(II) complex
Catecholase activity
Electrochemical analysis

ABSTRACT

This work presents the synthesis of an unprecedented *p*-cresol-conjugated copper(II) complex as a *p*-cresol-coupled polydentate ligand, its crystal structure, and catecholase activity. X-ray crystallography reveals that the Cu(II) centre adopts a nearly planar coordination geometry. Crystal data for $C_{14}H_{13}Cu_{0.5}O_3$: Monoclinic, space group $P2_1/c$ (no. 14), a = 5.9204(2) Å, b = 21.5615(10) Å, c = 9.0715(4) Å, β = 91.266(4)°, V = 1157.72(8) Å^3, Z = 4, μ(MoKα) = 0.987 mm^{-1}, *Dcalc* = 1.498 g/cm^3, 12647 reflections measured (6.884° ≤ 2Θ ≤ 63.42°), 3233 unique (R_{int} = 0.0618, R_{sigma} = 0.0512) which were used in all calculations. The final R_1 was 0.0710 (I > 2σ(I)) and wR_2 was 0.2173 (all data). The crystallized *p*-cresol was localized in complex units through intermolecular O···H interactions and formed a 3D supramolecular framework employing short-ranged O···H and C-H···π interactions in the solid state. The copper(II) complex has been evaluated as a bioinspired catalyst in the oxidative transformation of 3,5-di-*tert*-butylcatechol (DTBC) to *o*-benzoquinone in acetonitrile with a high turnover number, 2.26×10^4 h^{-1}. Electrochemical analysis of the copper(II) complex in the presence of DTBC recommends the generation of a catechol/*o*-benzosemiquinone redox couple during catalytic oxidation with the generation of hydrogen peroxide as a byproduct.

Cite this: *Eur. J. Chem.* **2023**, *14(4)*, 499-506 **Journal website**: www.eurjchem.com

1. Introduction

Copper is one of the precious biometals, principally for its significant contributions to biological processes and its captivating synergism with therapeutics [1,2]. Copper plays a pivotal role in cell physiology as a catalytic cofactor in the redox events of mitochondrial respiration, free radical scavenging, iron absorption, and elastin crosslinking [3-5]. Among the numerous activities of copper ions in biological applications, copper-mediated enzymatic activities have attracted a large amount of interest among synthetic coordination chemists. In this view, the catecholase enzyme, a copper-centric bioenzyme, catalyzes the transformation of *o*-diphenols into orthoquinones by coupling with oxygen. *o*-Diphenols exists in various plant and fungal species [6,7]. In plants, catecholase plays a crucial role in the oxidative transformation of catechol to *o*-quinone, leading to the development of brown-colored melanin through rapid polymerization [8,9].

In contrast, the potential coordinating characteristics of salicylaldehyde and its coupling with earth-abundant metal complexes arouse great promise in the discovery of numerous applications in both pure and applied chemistry [10,11]. The literature survey shows that salicylaldehyde has antimicrobial properties [12] and is known as a bidentate coordinator of *d* elements in monoanionic form, adopting a diversified coordination with metal centers [13].

In the biological world, copper ions in the coordination of various bio-ligands exist in the functional core of different metalloproteins [14,15]. At present, different scientific groups are actively engrossed in the catalytic oxidation of organic substrates based on synthetic copper(II)-based coordination compounds [16,17]. Focusing on the importance of the copper complexes, a newly designed copper(II) complex with structural characterization is reported with the efficient biomimicking activities of catecholase in this study.

2. Experimental

2.1. Preparation of the complex

2.1.1. Chemicals, solvents, and starting materials

Highly pure salicylaldehyde (Alfa Aeser, UK), morpholine, *p*-cresol (Merck, India), copper acetate monohydrate (Thomas Baker, India), and other chemicals of analytical grade were purchased from commercial outlets.

https://dx.doi.org/10.5155/eurjchem.14.4.499-506.2489

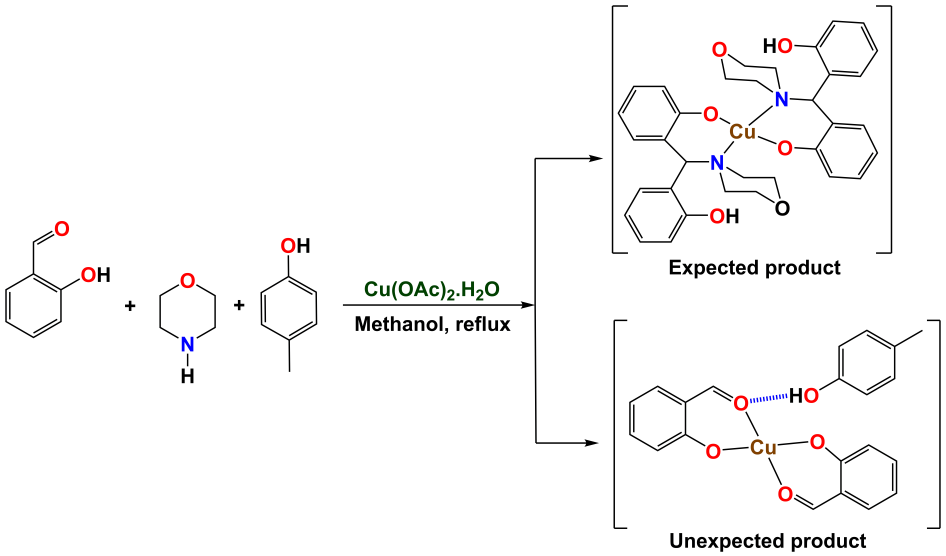

Scheme 1. Synthetic route for the copper(II) complex.

2.1.2. General procedure for the synthesis of copper(II) complex

The Cu complex (**1**) was prepared by an *in situ* reaction with salicylaldehyde in the presence of morpholine and *p*-cresol with the objective of designing a Mannich base ligand. A methanolic solution of salicylaldehyde (0.122 g, 1 mmol), morpholine (0.087 g, 1 mmol) and *p*-cresol (0.108 g, 1 mmol) was taken in a 100 mL two-neck round-bottom flask and refluxed for 6 hours. Subsequently, a solution of $Cu(OAc)_2$ (0.199 g, 1 mmol) in CH_3OH was added to the reaction mixture and the whole solution was refluxed again for 3 hours. When the reaction mixture was cooled for an hour, the crystalline copper complex was separated from the reaction mixture. The crystalline product was collected and stored in a vacuum desiccator.

Bis-(2-Formylphenolato)Copper(II) 4-methylphenol (**1**): Color: Greenish brown. Yield: 86.4%. FT-IR (KBr, ν, cm^{-1}): 3456 (OH, Phenolic-OH), 1605 (C=O, (Aldehyde). Anal. calcd. for $C_{21}H_{18}O_5Cu$ (**1**): C, 60.94; H, 4.38; O, 19.33; Found: C, 60.96; H, 4.36; O, 19.31%. UV/Vis ($CHCl_3$, λ_{max}, nm, (ε)): 315 (0.149), 382 (0.09).

2.2. Instrumentation

The IR spectrum of the copper complex was recorded in 400-3600 cm^{-1} using an FTIR-8400S Shimadzu spectrometer (Shimadzu, Kyoto, Japan). A Hitachi U-2910 UV-vis spectrophotometer (Hitachi, Japan) was used to measure the UV-vis spectra. A PerkinElmer 2400 CHN microanalyzer (Perkin Elmer, Waltham, USA) was used to record the elemental analysis. The electroanalytical instrument, PG Lyte1.0 was used to recode the cyclic voltammograms in acetonitrile. The platinum working electrode, platinum auxiliary electrode, and Ag/AgCl reference electrode were used for the measurements.

2.3. X-ray diffraction study

X-ray crystallography analysis of the Cu complex was performed on a Rigaku XtaLAB Mini diffractometer equipped with a Mercury 375R (2×2 bin mode) CCD detector. Data were collected with graphite monochromated Mo-Kα radiation (λ = 0.71073 Å) at 293(2) K using ω scans. Data were reduced using CrysAlisPro 1.171.39.35c [18] and the determination of the space group was made using Olex2. The structure was resolved using the dual space method using SHELXT-2015 [19] and refined using full-matrix least squares procedures using the SHELXL-2015 [20] software package through the OLEX2 suite [21].

2.4. Catecholase activity of the copper(II) complex

The catecholase activity was studied by treatment of 1×10^{-4} M solution of the Cu(II) complex with 1×10^{-3} M 3,5-di-*tert*-butylcatechol (DTBC) in acetonitrile (ACN) under an aerobic atmosphere. The change in absorbance with wavelength (wavelength scans) of the solution was monitored spectrophotometrically within 300-800 nm at an interval of 5 minutes [22].

Kinetic experiments were also performed with a spectrophotometer to determine the efficiency of catalytic oxidation of DTBC by the Cu(II) complex in ACN [22]. The kinetics of the catalytic transformation of 3,5-DTBC were performed following the initial rate method. Catalytic oxidation was monitored as a function of time with the growth of *o*-benzoquinone species at 400 nm [23]. ~1×10^{-3} M solution of the copper complex was mixed with a 1×10^{-2} M solution of DTBC and the conversion of DTBC to 3,5-di-*tert*-*o*-butylquinone was monitored by time scan at a wavelength of 400 nm in ACN. Kinetic analyzes were performed in triplicate to reveal the rate and efficiency of the catalytic oxidation reaction. The involvement of aerobic oxygen in the oxidation of DTBC was examined in the presence of hydrogen peroxide following a reported procedure [24].

3. Results and discussion

3.1. Design, synthesis and formulation of the copper(II) complex (1)

The Cu complex was formed by an *in situ* reaction with salicylaldehyde in the presence of morpholine and *p*-cresol. Initially, we intended to form a Mannich base ligand using salicylaldehyde, morpholine and *p*-cresol (1: 1: 1) refluxed in methanol for 6 hours and a methanolic solution of $Cu(OAc)_2$ (1 mmol) was added and the mixture was refluxed again for 3 hours. The synthetic route is shown in Scheme 1. After the analysis of the XRD study, we found that the expected ligand was not formed and Cu-acetate formed an inner metallic complex with two units of salicylaldehyde.

Table 1. Crystal data and structure refinement for the copper(II) complex (**1**).

Empirical formula	$C_{28}H_{26}CuO_6$
Formula weight (g/mol)	261.01
Temperature (K)	293(2)
Crystal system	Monoclinic
Space group	$P2_1/c$
a, (Å)	5.9204(2)
b, (Å)	21.5615(10)
c, (Å)	9.0715(4)
β (°)	91.266(4)
Volume (Å^3)	1157.72(8)
Z	2
ρ_{calc} (g/cm^3)	1.498
μ (mm^{-1})	0.987
F(000)	542.0
Crystal size (mm^3)	0.4 × 0.6 × 0.2
Radiation	MoKα (λ = 0.71073)
2Θ range for data collection (°)	6.884 to 63.42
Index ranges	$-7 \le h \le 8$, $-30 \le k \le 27$, $-12 \le l \le 10$
Reflections collected	12647
Independent reflections	3233 [R_{int} = 0.0618, R_{sigma} = 0.0512]
Data/restraints/parameters	3233/0/162
Goodness-of-fit on F^2	1.144
Final R indexes [I≥2σ (I)]	R_1 = 0.0710, wR_2 = 0.2120
Final R indexes [all data]	R_1 = 0.0812, wR_2 = 0.2173
Largest diff. peak/hole (e.Å^{-3})	0.83/-1.37

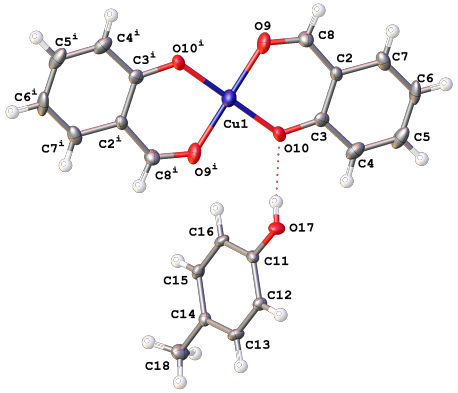

Figure 1. Thermal ellipsoidal plots of the copper(II) complex.

The *p*-cresol unit is situated in close proximity to the complex part by noncovalent interaction. The copper(II) complex is found to be soluble in polar solvents such as CH_3OH, C_2H_5OH, and CH_3CN, *etc*.

The significant deviation from the targeted Mannich base product may be explained in terms of the acid-base chemistry of the reactants involved. The literature survey shows that the p*K*a values for salicylaldehyde and *p*-cresol are 8.22 and 10.37 [25] in typical cases, attributed to the relatively higher acidity of salicylaldehyde. This report on acidity for salicylaldehyde offers a better delivery of protons to morpholine (a 2° amine), resulting in the deactivation of the nucleophilic character of the amine in its proton-abstracted form. When the copper salt was added *in situ*, a stable copper chelate was formed with the anionic salicylaldehyde. The *p*-cresol turns out to be a crystallized molecule in the formation of a crystalline copper complex, as revealed by X-ray crystallography through its active participation in the short-ranged hydrogen bonding with the complex without any permanent binding.

3.2. Description of crystal structure and supramolecular interactions

X-ray diffraction analysis reveals that a mononuclear copper(II) complex unit cocrystallizes with a *p*-methyl phenol in a monoclinic system adopting a $P2_1/c$ space group. The copper(II) centre has a nearly square planar coordination geometry, as evidenced by the measurement of crystallographic bond angles. The slight distortion to the square plane appears through the chelating angles of the salicylaldehyde ligand. The crystallographic refinement parameter is summarized in Table 1. Bond distances and bond angles for copper(II) complex are given in Tables 2 and 3, respectively. The thermal ellipsoidal plot of the Cu complex is shown in Figure 1.

Self-assembly analysis shows a notable presence of *p*-methyl phenol along with the copper(II) complex in the crystalline framework. In the crystalline architecture of the copper complex, the crystallized *p*-cresol forms a very strong intermolecular H-bonding network with the copper complex ranging from 2.00 to 2.795 Å (O17-H17···O10). Investigation of the self-assembly of the copper complex exhibits non-covalent interactions such as O···H and C-H···π (Table 4) is responsible for the network formation. The mononuclear copper(II) complex interacts with another complex unit through strong O···H and C-H···π and seems to be a complex dimer (Figure 2).

The Hirshfeld surface analysis of the copper(II) complex over a definite d_{norm} was calculated with Crystal Explorer 21 software [26]. Surface volume and area are calculated as 281.68 Å^3 and 282.63 Å^2. The red highlighted spots indicate the d_{norm} area and present close noncovalent interactions in the copper complex with the -OH group of the *p*-cresol unit (Figure 3a). The contribution of each element in the noncovalent interactions is given in Table 5. The blue area in the d_{norm} cites important C-H···π interactions between the phenyl centroid and the H of the C attached to the phenyl and methyl groups. White areas denote no interaction. The interactions in the copper(II) complex are obtained from fingerprint plots (Table 5, Figure 4).

Table 2. Bond distances for copper(II) complex (1).

Atom	Atom	Length, Å	Atom	Atom	Length, Å
Cu1	O10	1.928(3)	C11	C12	1.390(5)
Cu1	O10[1]	1.928(3)	C2	C8	1.423(5)
Cu1	O9	1.899(3)	C2	C7	1.421(5)
Cu1	O9[1]	1.899(3)	C15	C14	1.393(5)
O10	C3	1.312(4)	C7	C6	1.379(6)
O17	C11	1.365(4)	C18	C14	1.510(5)
O9	C8	1.245(5)	C13	C14	1.395(5)
C16	C11	1.397(5)	C13	C12	1.398(5)
C16	C15	1.391(5)	C5	C4	1.379(6)
C3	C2	1.418(5)	C5	C6	1.402(6)
C3	C4	1.415(5)			

[1]1-*x*, 1-*y*, 2-*z*.

Table 3. Bond angles for copper(II) complex (1).

Atom	Atom	Atom	Angle, °	Atom	Atom	Atom	Angle, °
O10	Cu1	O10[1]	180.0	C3	C2	C8	122.3(3)
O9[1]	Cu1	O10	86.45(11)	C3	C2	C7	120.8(3)
O9	Cu1	O10[1]	86.45(12)	C7	C2	C8	117.0(3)
O9[1]	Cu1	O10[1]	93.55(12)	C16	C15	C14	121.6(3)
O9	Cu1	O10	93.55(12)	O9	C8	C2	127.5(3)
O9	Cu1	O9[1]	180.0	C6	C7	C2	120.5(4)
C3	O10	Cu1	126.2(2)	C14	C13	C12	120.9(3)
C8	O9	Cu1	126.3(3)	C15	C14	C18	120.7(3)
C15	C16	C11	119.6(3)	C15	C14	C13	118.1(3)
O10	C3	C2	123.8(3)	C13	C14	C18	121.1(3)
O10	C3	C4	119.0(3)	C4	C5	C6	121.7(4)
C4	C3	C2	117.2(3)	C5	C4	C3	121.1(4)
O17	C11	C16	122.8(3)	C7	C6	C5	118.8(4)
O17	C11	C12	117.6(3)	C11	C12	C13	120.1(3)
C12	C11	C16	119.6(3)				

[1]1-*x*, 1-*y*, 2-*z*.

Table 4. Hydrogen bond and C–H···π interaction parameters for copper(II) complex (Å, °).

D-H···A	D-H	H···A	D···A	∠ D-H···A	Symmetry code
O17–H17···O10	0.8200	2.0000	2.795(4)	165.00	1-*x*, -1/2+*y*, 3/2-*z*
X-H···Cg	**H···Cg**		**X···Cg**	**∠ X-H···Cg**	**Symmetry code**
C(6)-H(6)···Cg(4)	2.83		3.487(4)	129	2-*x*, 1-*y*, 1-*z*
C(18)-H(18B)···Cg(4)	2.99		3.570(4)	120	*x*, 1/2-*y*, -1/2+*z*

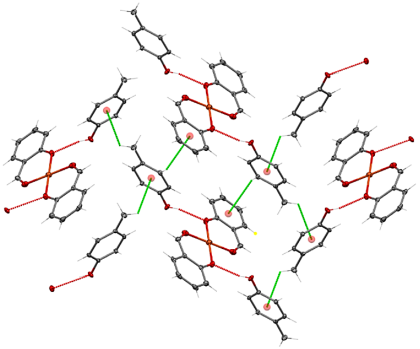

Figure 2. *p*-Cresol mediated the supramolecular framework of the copper(II) complex through O···H and C–H···π interactions.

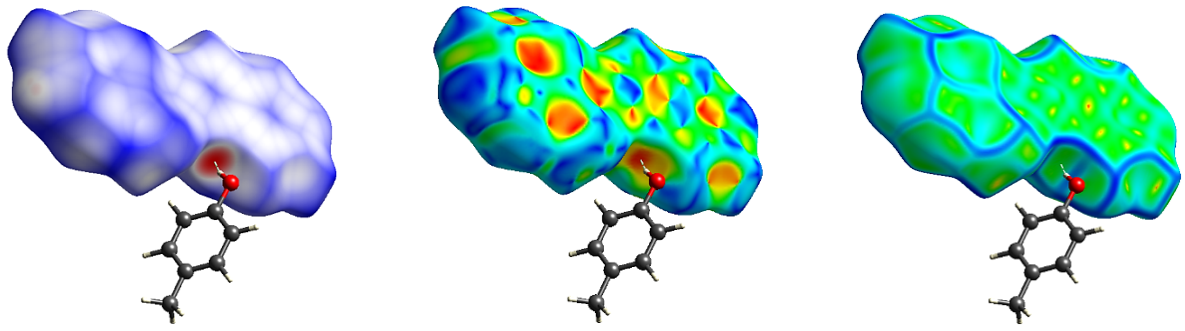

(a) (b) (c)

Figure 3. (a) The red highlighted spots indicate the d_{norm} area with the closest non-covalent interactions in the copper(II) complex with the -OH group of *p*-cresol unit, (b) Hirshfeld Surface shape index indicating the HS flatness or curvature and (c) Curvedness of the surface indicating concavity or convexity of the Hirshfeld Surface.

Table 5. Percentage share of the interaction of each atom with other atoms when they are in or out of the Hirshfeld surface for copper(II) complex.

Inside	Outside	% Surface area included	Inside	Outside	% Surface area included
All	All	100.0	Cu	O	0.0
All	Cu	2.6	C	C	3.4
All	C	17.9	C	H	13.1
All	H	67.9	C	O	4.3
All	O	11.6	H	H	40.3
Cu	C	2.6	H	O	7.2
Cu	H	0.1	O	O	0.1

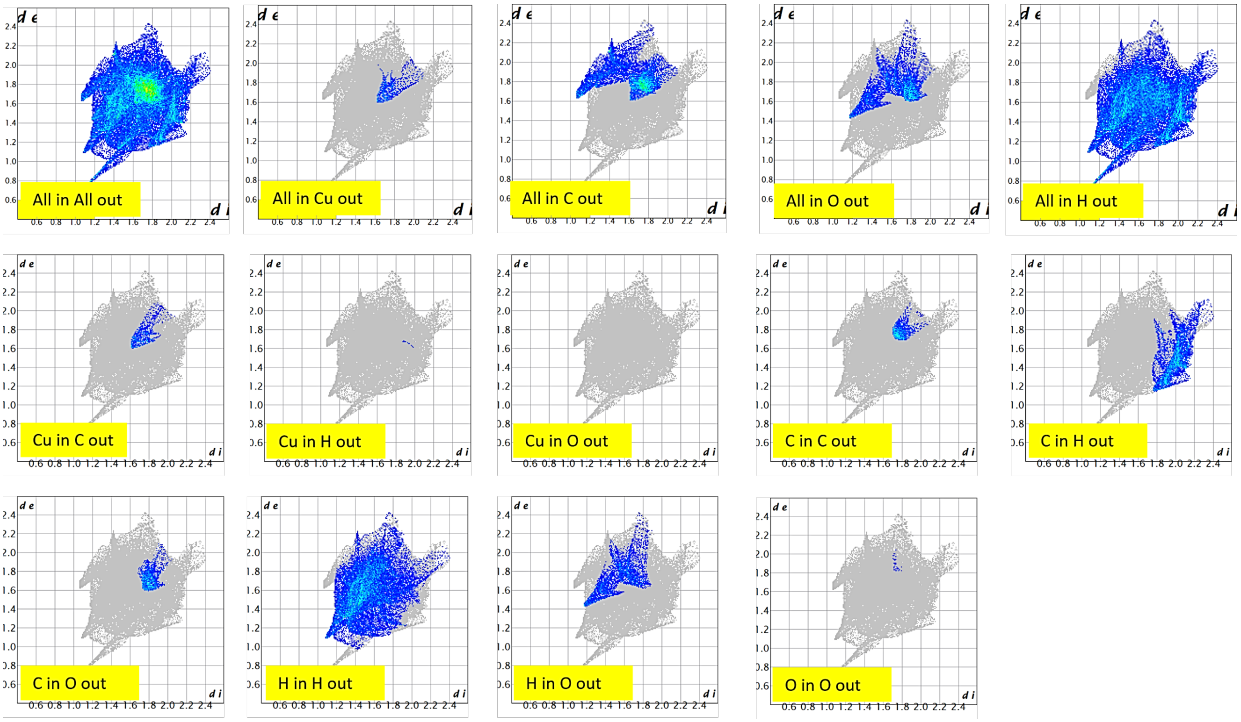

Figure 4. 2-Dimensional fingerprint plots of the copper(II) complex (1).

3.3. Solution property of the copper(II) complex

The Cu(II) complex displayed the electronic bands at 315 and 382 nm in ACN at room temperature. The electronic bands at 315 and 382 nm in the complex can be assigned to the presence of π → π* and charge transfer (CT) transitions, respectively [2,3].

3.4. Catecholase activity of the copper(II) complex

The catecholase-mimicking activity of the synthetic copper(II) complex has been examined by considering 3,5-DTBC as a model substrate. DTBC contains two bulky *t*-butyl substituents at the phenyl ring and helps to lower the quinone-catechol reduction potential. The low quinone-catechol reduction potential facilitates the oxidation of catechol to the corresponding *o*-quinone, DTBQ under ambient reaction conditions (Scheme 2). It is well documented that DTBQ is quite stable in solution and displays a characteristic absorption peak at 401 nm in acetonitrile [3].

The nature of the changes in the spectral bands during catalytic oxidation was monitored with a UV-vis spectrophotometer for a 1.5 h period (Figure 5). The copper complex displays a characteristic electronic transition at 378 nm. Upon the addition of the Cu(II) complex to the DTBC solution, a new electronic band at 400 nm started to develop with increasing absorbance (Figure 5). The rise of the optical band at 400 nm is a definite signature of the oxidation of DTBC in ACN. Interestingly, a new optical band also appeared at 551 nm with a decrease of the absorbance for the electronic band at 700 nm. The appearance and disappearance of the electronic bands occurred through the existence of an isobestic point at 605 nm, ensuring an equilibrium between the copper complex-DTBC adducts and the copper complex-semibenzoquinonate species [6,27]. The appearance of this new electronic band at 400 nm in the spectrophotometric scan is assigned to the production of *o*-benzoquinone species in ACN.

The kinetics of the catalytic oxidation of DTBC was studied to determine the catalytic performance of the copper(II) complex. The kinetic parameter of the catalytic oxidation of DTBC was evaluated employing the method of the initial rate. The growth of *o*-benzoquinone was monitored as a function of time with respect to 400 nm (Figure 5) [25]. The nature of oxidation kinetics was examined by plotting the rate constants *vs.* the concentration of DTBC as shown in Figure 5. The first-order saturation kinetics of the oxidation reaction seems to be suitable in the Michaelis–Menten model and can be expressed as Equation (1):

$$V = \frac{V_{max}\,[S]}{K_M + [S]} \quad (1)$$

where V indicates the rate of the oxidation reaction, K_m denotes the Michaelis-Menten constant, V_{max} presents the maximum velocity of the reaction, and [*S*] is the concentration of the DTBC.

The values of the kinetic parameters were determined from the Michaelis-Menten equation as V_{max} (MS^{-1}) = 6.26×10^{-4}; K_M = 3.80×10^{-3} [Std. error for V_{max} (MS^{-1}) = 3.40×10^{-5}; Std. error for K_m (M)= 5.49×10^{-4}].

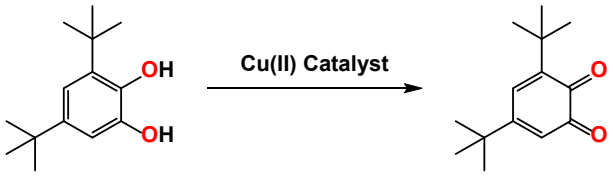

Scheme 2. Catalytic oxidation of DTBC to DTBQ.

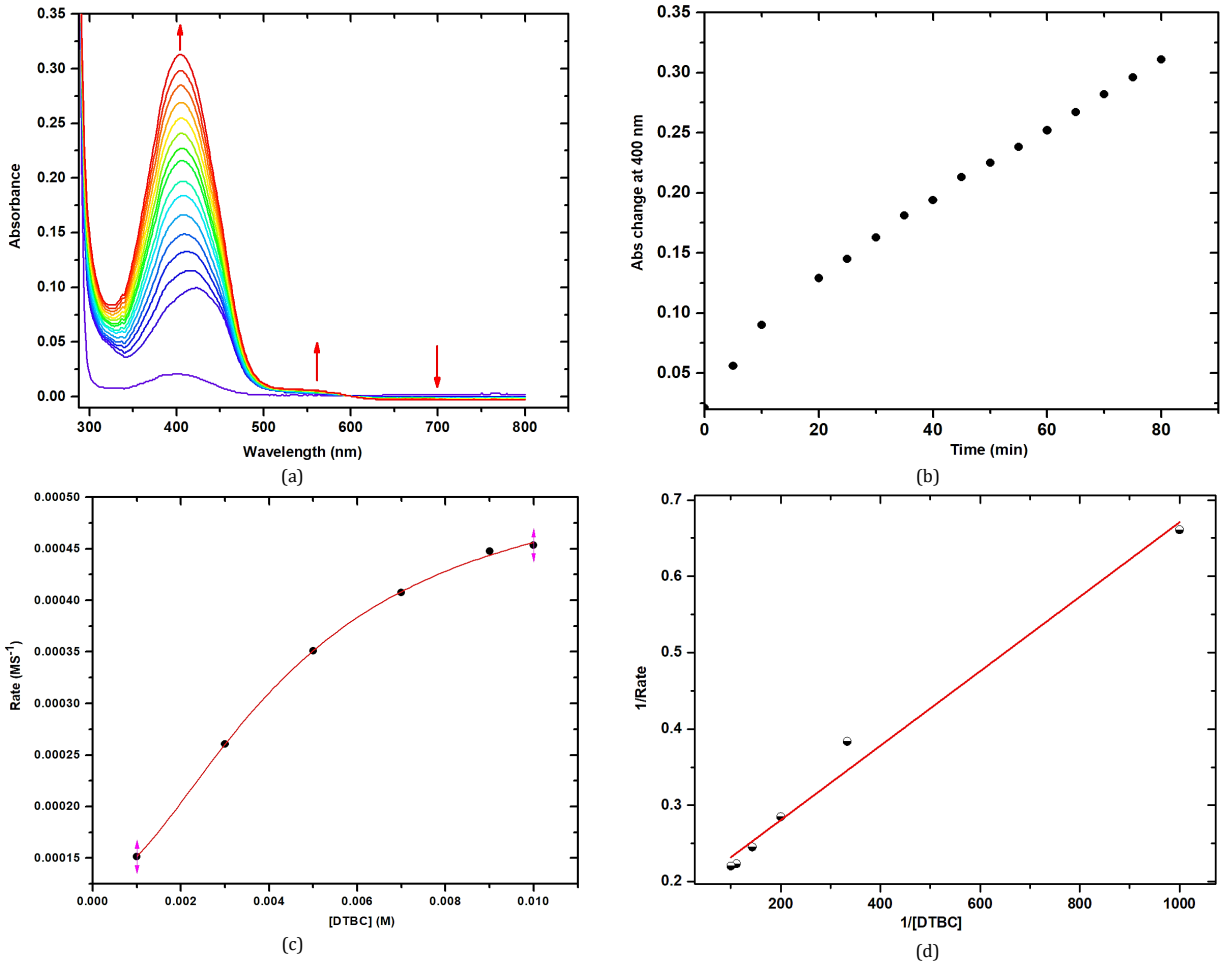

Figure 5. (a) Rise of a new electronic band at 400 nm after addition of DTBC to the copper (II) complex in ACN with a time interval of 5 min, (b) Time *vs* absorbance plot at 400 nm, (c) Rate *vs* [DTBC] plot and (d) 1/Rate *vs* 1/DTBC plots.

The catalyst turnover number for the catalyst was found to be 2.26×10^4 h^{-1}. The catalytic efficiency for the catalytic oxidation of DTBC was determined as $k_{cat}/K_M = 5.94\times10^5$.

The redox activities of the copper complex and its activities toward the biomimetics of catecholase activities were studied by electrochemical analysis in CH_3CN at 295 K. The redox behavior of the copper complex was recorded using Ag/AgCl reference under an aerobic atmosphere. The cyclic voltammograms are illustrated in Figure 6. The copper(II) complex exhibits two distinct cathodic waves at -0.97 and -1.18 V, corresponding to Cu^{2+}/Cu^{+} and Cu^{+}/Cu^{0} redox couples, respectively, in solution. Notably, the appearance of the anodic waves at +1.37 and +1.56 V can be attributed to the phenoxide/phenoxide anion radical ($O^{-}/O^{\cdot-}$) redox couples of the chelated-salicylaldehyde in the copper and free *p*-cresol co-crystallized with the complex. The catecholase activity was authenticated by the change in cyclic voltammograms of the copper complex upon sequential addition of DTBC in CH_3CN at 295 K. Cyclic voltammograms of the copper complex after gradual addition of DTBC displayed the shift of the cathodic wave at -1.18 to -1.61 V, while the wave at -0.97 V due to Cu(II)/Cu(I) species gets diminished. In contrast, the replicate cathodic waves at -0.45 V and the replicate anodic peak at 0.45 V newly appeared which is assignable to the cat/sq redox couple (cat = catechol, sq = *o*-benzosemiquinone and isq = *o*-iminobenzosemiquinone). This peak is a definite sign of the oxidation of DTBC. The disappearance of the Cu^{2+}/Cu^{+} peak indicates the involvement of Cu^{2+} in the oxidation processes [5].

Further, the chemical fate of molecular oxygen in the participation of DTBC oxidation was assessed from the production of hydrogen peroxide [28]. An electronic band at λ_{max} 351 nm established the presence of hydrogen peroxide in the oxidation of DTBC and thus confirmed the reduction of oxygen to H_2O_2 in the course of the oxidation. Furthermore, the durability of the copper(II) catalyst was consolidated in the oxidative transformation of DTBC by correlating the UV-vis spectrum of the solution after isolating the oxidation product.

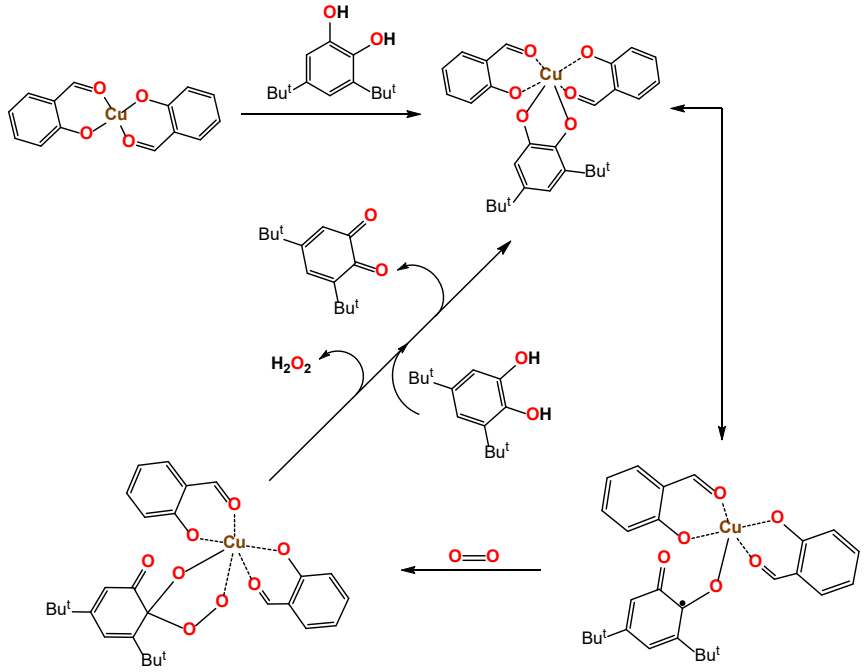

Scheme 3. Plausible mechanistic cycle for catecholase activity of the copper(II) complex.

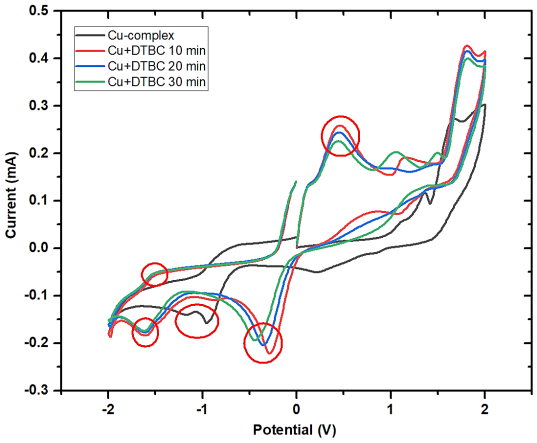

Figure 6. Cyclic voltammogram of the copper(II) complex with sequential addition of DTBC in CH_3CN under aerobic conditions.

The solution containing the copper complex as a catalyst produces types of electronic bands at 315 and 382 nm similar to the electronic bands of the original copper complex displayed in ACN and ensures the durability of the catalyst in DTBC oxidation. Therefore, based on the experimental results, a plausible mechanistic cycle for the catalytic oxidation of DTBC may be proposed according to Scheme 3.

4. Conclusions

This research work deals with the synthesis, crystal structure, and biomimetics of catecholase activity of the copper(II) complex. The copper(II) centre adopts a nearly perfect square planar geometry and coexists with *p*-cresol in the solid state through an intermolecular hydrogen bonding interaction. The deviation from the formation of the Mannich base can be explained in terms of acid-base chemistry and, under the reaction condition, upon in situ addition of the copper salt leads to the generation of the copper(II) complex where the *p*-cresol supports the crystallization of the complex. The copper(II) complex exhibits excellent catalytic oxidation activity, denoted by $k_{cat}/K_{M,}$ which is found to have the value of 5.94×10^5. Electrochemical and spectrophotometric spectral studies of the Cu(II) complex in the presence of DTBC suggest the development of an isobestic point at ~595 nm that represents the transformation of the Cu(II) complex-DTBC adduct into Cu(II) complex-DTBSQ species in solution. Cyclic voltammogram analysis confirms the presence of semiquinone at +0.45 V and offers a new addition of the copper complex that effectively mimics catecholase functionality.

Acknowledgements

Dr. Bhaskar Biswas gratefully acknowledges the financial support received from the University of North Bengal, Darjeeling 734013, India.

Supporting information

CCDC-2299271 contains the supplementary crystallographic data for this paper. These data can be obtained free of charge via www.ccdc.cam.ac.uk/data request/cif, or by e-mailing data request@ccdc.cam.ac.uk, or by contacting The Cambridge Crystallographic Data Centre, 12 Union Road, Cambridge CB2 1EZ, UK; fax: +44(0)1223-336033.

Disclosure statement

Conflict of interest: The authors declare that they have no conflict of interest.
Author contributions: All authors contributed equally to this work.
Ethical approval: All ethical guidelines have been adhered.
Sample availability: Samples of the compounds are available from the author.

CRediT authorship contribution statement

Conceptualization: Subham Mukherjee, Bhaskar Biswas; Methodology: Subham Mukherjee, Gayetri Sarkar; Validation: Subham Mukherjee, Gayetri Sarkar; Abhranil De; Formal Analysis: Subham Mukherjee, Gayetri Sarkar; Abhranil De; Investigation: Subham Mukherjee, Gayetri Sarkar; Abhranil De; Resources: Subham Mukherjee, Bhaskar Biswas; Data Curation: Subham Mukherjee, Gayetri Sarkar; Abhranil De; Writing - Original Draft: Subham Mukherjee, Bhaskar Biswas; Writing - Review and Editing: Bhaskar Biswas.

ORCID and Email

Subham Mukherjee
smukherjee@suryasencollege.org.in
https://orcid.org/0000-0002-1541-2839
Gayetri Sarkar
iamgayetri007@gmail.com
https://orcid.org/0009-0008-9729-9331
Abhranil De
abhranilde@gmail.com
https://orcid.org/0000-0003-2266-9023
Bhaskar Biswas
bhaskarbiswas@nbu.ac.in
mr.bbiswas@rediffmail.com
https://orcid.org/0000-0002-5447-9729

References

[1]. Debnath, A.; Diyali, S.; Das, M.; Panda, S. J.; Mondal, D.; Dhak, D.; Purohit, C. S.; Ray, P. P.; Biswas, B. Harnessing the hydrogen evolution reaction (HER) through the electrical mobility of an embossed Ag(i)-molecular cage and a Cu(ii)-coordination polymer. *Dalton Trans.* **2023**, *52*, 8850–8856.
[2]. Kundu, S.; Saha, S.; Panda, S. J.; Purohit, C. S.; Biswas, B. Tailor-made isostructural copper(ii) and nickel(ii) complexes with a newly designed (*N*,*N*)-donor scaffold as functional mimics of alkaline phosphatase. *New J Chem* **2023**, *47*, 5894–5902.
[3]. Mudi, P. K.; Mahato, R. K.; Joshi, M.; Shit, M.; Choudhury, A. R.; Das, H. S.; Biswas, B. Copper(II) complexes with a benzimidazole functionalized Schiff base: Synthesis, crystal structures, and role of ancillary ions in phenoxazinone synthase activity. *Appl. Organomet. Chem.* **2021**, *35*, e6211.
[4]. Garai, M.; Dey, D.; Yadav, H. R.; Choudhury, A. R.; Maji, M.; Biswas, B. Catalytic fate of two copper complexes towards phenoxazinone synthase and catechol dioxygenase activity. *ChemistrySelect* **2017**, *2*, 11040–11047.
[5]. Tapiero, H.; Townsend, D. M.; Tew, K. D. Trace elements in human physiology and pathology. Copper. *Biomed. Pharmacother.* **2003**, *57*, 386–398.
[6]. Gerdemann, C.; Eicken, C.; Krebs, B. The crystal structure of catechol oxidase: New insight into the function of type-3 copper proteins. *Acc. Chem. Res.* **2002**, *35*, 183–191.
[7]. Halder, J.; Tamuli, P.; Bhaduri, A. N. Isolation and characterization of polyphenol oxidase from Indian tea leaf (Camellia sinensis). *J. Nutr. Biochem.* **1998**, *9*, 75–80.
[8]. Koval, I. A.; Gamez, P.; Belle, C.; Selmeczi, K.; Reedijk, J. Synthetic models of the active site of catechol oxidase: mechanistic studies. *Chem. Soc. Rev.* **2006**, *35*, 814–840.
[9]. Drewry, J. A.; Gunning, P. T. Recent advances in biosensory and medicinal therapeutic applications of zinc(II) and copper(II) coordination complexes. *Coord. Chem. Rev.* **2011**, *255*, 459–472.
[10]. Sorenson, J. R. J. 6 copper complexes offer a physiological approach to treatment of chronic diseases. In *Progress in Medicinal Chemistry*; Elsevier, 1989; pp. 437–568.
[11]. Jayamani, A.; Sengottuvelan, N.; Chakkaravarthi, G. Synthesis, structural, electrochemical, DNA interaction, antimicrobial and molecular docking studies on dimeric copper(II) complexes involving some potential bidentate ligands. *Polyhedron* **2014**, *81*, 764–776.
[12]. Elo, H.; Kuure, M.; Pelttari, E. Correlation of the antimicrobial activity of salicylaldehydes with broadening of the NMR signal of the hydroxyl proton. Possible involvement of proton exchange processes in the antimicrobial activity. *Eur. J. Med. Chem.* **2015**, *92*, 750–753.
[13]. Costa Pessoa, J.; Cavaco, I.; Correia, I.; Tomaz, I.; Duarte, T.; Matias, P. M. Oxovanadium(IV) complexes with aromatic aldehydes. *J. Inorg. Biochem.* **2000**, *80*, 35–39.
[14]. Solomon, E. I.; Heppner, D. E.; Johnston, E. M.; Ginsbach, J. W.; Cirera, J.; Qayyum, M.; Kieber-Emmons, M. T.; Kjaergaard, C. H.; Hadt, R. G.; Tian, L. Copper active sites in biology. *Chem. Rev.* **2014**, *114*, 3659–3853.
[15]. Solomon, E. I.; Baldwin, M. J.; Lowery, M. D. Electronic structures of active sites in copper proteins: contributions to reactivity. *Chem. Rev.* **1992**, *92*, 521–542.
[16]. Punniyamurthy, T.; Rout, L. Recent advances in copper-catalyzed oxidation of organic compounds. *Coord. Chem. Rev.* **2008**, *252*, 134–154.
[17]. Selmeczi, K.; Réglier, M.; Giorgi, M.; Speier, G. Catechol oxidase activity of dicopper complexes with N-donor ligands☆. *Coord. Chem. Rev.* **2003**, *245*, 191–201.
[18]. Agilent (2017). CrysAlis PRO. Agilent Technologies Ltd, Yarnton, Oxfordshire, England.
[19]. Sheldrick, G. M. *SHELXT*– Integrated space-group and crystal-structure determination. *Acta Crystallogr. A Found. Adv.* **2015**, *71*, 3–8.
[20]. Sheldrick, G. M. Crystal structure refinement with *SHELXL*. *Acta Crystallogr. C Struct. Chem.* **2015**, *71*, 3–8.
[21]. Dolomanov, O. V.; Bourhis, L. J.; Gildea, R. J.; Howard, J. A. K.; Puschmann, H. *OLEX2*: a complete structure solution, refinement and analysis program. *J. Appl. Crystallogr.* **2009**, *42*, 339–341.
[22]. Mukherjee, S.; Pal, C. K.; Kotakonda, M.; Joshi, M.; Shit, M.; Ghosh, P.; Choudhury, A. R.; Biswas, B. Solvent induced distortion in a square planar copper(II) complex containing an azo-functionalized Schiff base: Synthesis, crystal structure, in-vitro fungicidal and anti-proliferative, and catecholase activity. *J. Mol. Struct.* **2021**, *1245*, 131057.
[23]. Dey, D.; De, A.; Yadav, H. R.; Guin, P. S.; Choudhury, A. R.; Kole, N.; Biswas, B. An oxido-bridged diiron(II) complex as functional model of catechol dioxygenase. *ChemistrySelect* **2016**, *1*, 1910–1916.
[24]. De, A.; Dey, D.; Yadav, H. R.; Maji, M.; Rane, V.; Kadam, R. M.; Choudhury, A. R.; Biswas, B. Unprecedented hetero-geometric discrete copper(II) complexes: Crystal structure and bio-mimicking of Catecholase activity. *J. Chem. Sci. (Bangalore)* **2016**, *128*, 1775–1782.
[25]. Liptak, M. D.; Gross, K. C.; Seybold, P. G.; Feldgus, S.; Shields, G. C. Absolute p*K*a determinations for substituted phenols. *J. Am. Chem. Soc.* **2002**, *124*, 6421–6427.
[26]. Spackman, P. R.; Turner, M. J.; McKinnon, J. J.; Wolff, S. K.; Grimwood, D. J.; Jayatilaka, D.; Spackman, M. A. *CrystalExplorer*: a program for Hirshfeld surface analysis, visualization and quantitative analysis of molecular crystals. *J. Appl. Crystallogr.* **2021**, *54*, 1006–1011.
[27]. De, A.; Garai, M.; Yadav, H. R.; Choudhury, A. R.; Biswas, B. Catalytic promiscuity of an iron(II)–phenanthroline complex. *Appl. Organomet. Chem.* **2017**, *31*, e3551.
[28]. Leussing, D. L.; Bai, K. S. N-Salicylideneglycinato complexes. Comparison with pyridoxal. *Anal. Chem.* **1968**, *40*, 575–581.